Ultra-high Q/V hybrid cavity for strong light-matter interaction

Donato Conteduca, Christopher Reardon, Mark G. Scullion, Francesco Dell'Olio, Mario N. Armenise, Thomas F. Krauss, and Caterina Ciminelli

Citation: APL Photonics **2**, 086101 (2017); doi: 10.1063/1.4994056
View online: http://dx.doi.org/10.1063/1.4994056
View Table of Contents: http://aip.scitation.org/toc/app/2/8
Published by the American Institute of Physics

Ultra-high Q/V hybrid cavity for strong light-matter interaction

Donato Conteduca,[1] Christopher Reardon,[2] Mark G. Scullion,[2,a] Francesco Dell'Olio,[1] Mario N. Armenise,[1] Thomas F. Krauss,[2] and Caterina Ciminelli[1,b]

[1]*Optoelectronics Laboratory, Politecnico di Bari, Via E. Orabona 4, 70125 Bari, Italy*
[2]*Photonics Group, Department of Physics, University of York, Heslington, York YO10 5DD, United Kingdom*

(Received 16 March 2017; accepted 3 July 2017; published online 1 August 2017)

The ability to confine light at the nanoscale continues to excite the research community, with the ratio between quality factor Q and volume V, i.e., the Q/V ratio, being the key figure of merit. In order to achieve strong light-matter interaction, however, it is important to confine a lot of energy in the resonant cavity mode. Here, we demonstrate a novel cavity design that combines a photonic crystal nanobeam cavity with a plasmonic bowtie antenna. The nanobeam cavity is optimised for a good match with the antenna and provides a Q of 1700 and a transmission of 90%. Combined with the bowtie, the hybrid photonic-plasmonic cavity achieves a Q of 800 and a transmission of 20%, both of which remarkable achievements for a hybrid cavity. The ultra-high Q/V of the hybrid cavity is of order of 10^6 $(\lambda/n)^{-3}$, which is comparable to the state-of-the-art of photonic resonant cavities. Based on the high Q/V and the high transmission, we demonstrate the strong efficiency of the hybrid cavity as a nanotweezer for optical trapping. We show that a stable trapping condition can be achieved for a single 200 nm Au bead for a duration of several minutes (t_{trap} > 5 min) and with very low optical power (P_{in} = 190 μW). [http://dx.doi.org/10.1063/1.4994056]

INTRODUCTION

Resonant cavities with a high ratio between the cavity Q-factor and the mode volume V afford strong and long-lasting energy confinement of light.[1–3] This confinement enhances the light-matter interaction and enables a number of interesting applications, e.g., in optical communications, quantum electrodynamics (QED),[4] enhanced spontaneous emission,[5] non-linear optics,[6] biosensing,[7] and optical trapping.[8] A high Q/V can be achieved either by increasing the Q, as in dielectric cavities, or by decreasing the V, as in plasmonic cavities.

For the dielectric case, ultra-high Q-factors have already been obtained with Whispering Gallery Mode (WGM) cavities[9] and with Photonic Crystal (PhC) cavities.[10] In particular, very high Q-factor values of the order of 10^7 have been demonstrated in the 2D PhC system, corresponding to a photon lifetime of 7.5 ns,[11] combined with a diffraction-limited mode volume $V \sim (\lambda/n)^3$. Plasmonic cavities afford much smaller mode volumes by confining the electromagnetic energy beyond the diffraction limit at the metal-dielectric interface.[12] Sub-wavelength mode volumes have been obtained down to $V \sim 10^{-4}$ $(\lambda/n)^3$.[13] Such plasmonic sub-wavelength confinement is intrinsically related to high metal losses, which limits the Q-factor to values well below 100, resulting in Q/V values of 10^5 $(\lambda/n)^{-3}$ at best and low transmission values.[14]

Several configurations for increasing the Q/V ratio have been investigated, amongst which the hybrid combination of dielectric and plasmonic confinement mechanisms appears to be the most

[a]Now at Fraunhofer Centre for Applied Photonics, 99 George Street, Glasgow G1 1RD, United Kingdom.
[b]E-mail: caterina.ciminelli@poliba.it

promising.[15–21] A number of such hybrid cavities have already been studied with the aim to decrease the optical losses with respect to the plasmonic cavities and to provide very low values of mode volume. As a result, Q/V values up to 10^7 $(\lambda/n)^{-3}$ [21,22] have been predicted by simulations, with the best experimental results reaching values of 10^5 $(\lambda/n)^{-3}$.[23] It is also worth noting that hybrid cavities maintain the nanoscale plasmonic hotspot which is advantageously situated in the low index medium and which makes the device suitable for applications in biosensing and optical trapping,[24,25] while the lower loss compared to plasmonic cavities reduces thermal effects, e.g., the effect of Brownian motion counteracting optical trapping.[26]

Here, we report on a 1D PhC nanobeam cavity vertically coupled to a bowtie nanoantenna. We achieve an ultra-high $Q/V > 10^6$ $(\lambda/n)^{-3}$ factor and experimentally observe a remarkable resonance transmission of $T > 20\%$, in good agreement with simulations. We calculate a high optical stability of $S > 10$, a trapping stiffness of $k \geq 40$ pN/(nm/W) and demonstrate the trapping of 200 nm Au beads for a very low input power ($P_{in} = 190$ μW).

DESIGN AND NUMERICAL RESULTS

Our 1D PhC dielectric microcavity is based on a silicon (Si) photonic wire surrounded by SiO_2 on all sides (Fig. 1). The wire is $W = 460$ nm wide and $h = 220$ nm thick. The cavity mirrors consist of a central section of $N = 3$ holes with the same radius $r = 130$ nm and period $\Lambda = 390$ nm and of two symmetrically tapered sections at both sides. The tapered sections have been designed to improve the matching between the nanowire mode and the Bloch mode in the photonic crystal section aiming at reducing the coupling loss and increasing the on-resonance transmission.[27,28] In order to realize the taper, we consider a number of tapered holes $N_t = 3$, with a period that gradually reduces from $\Lambda = 390$ nm to $\Lambda = 330$ nm and radius from $r = 130$ to $r = 90$ nm. We achieve a transmission value of $T = 90\%$. High on-resonant transmission of the dielectric cavity is essential for the strong confinement of energy in the cavity and to ensure that the transmission remains high even in the presence of the plasmonic cavity. The plasmonic part of the cavity then consists of a gold bowtie nanoantenna, placed above the centre of the PhC cavity. We add a spacer G between the PhC and the bowtie in order to reduce the optical losses (see S1 of the supplementary material for further details). We assume water as the surrounding medium to accommodate the optical trapping application.

For the simulation, we used the 3D Finite Element Method (FEM) (COMSOL ®), taking the dispersion of Si and SiO_2 and the water losses into account. Using a TE polarized mode and a SiO_2 spacer of $G = 130$ nm, we calculated a Q-factor of 1800 and an on-resonance transmission of $T = 93\%$ at $\lambda_r = 1562.01$ nm [Fig. 2(a)].

The Au bowtie nanoantenna then consists of two symmetric gold triangles separated by a gap s. The bowtie generates a strong confinement on resonance,[29] effectively funneling the light from the PhC cavity to the plasmonic hotspot. For the bowtie, we chose a thickness of $c = 30$ nm for the gold, dimensions of $b = 350$ nm for the base of each triangle, and $a = 220$ nm for

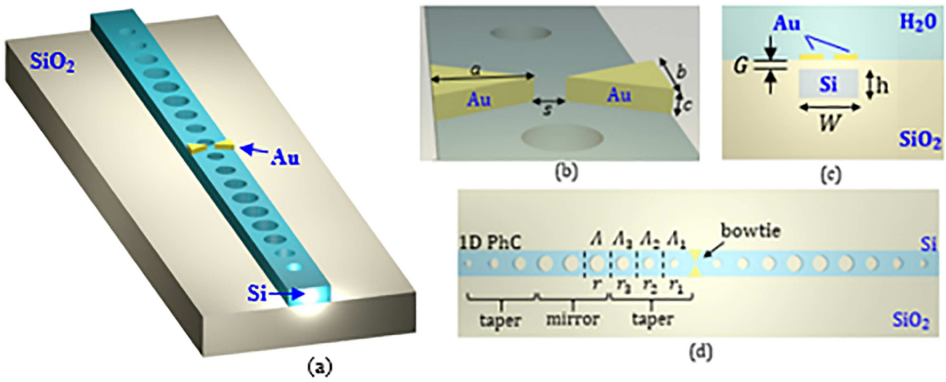

FIG. 1. (a) Overview of the hybrid cavity; (b) detail of the bowtie; (c) cross-section and (d) top-view of the hybrid cavity.

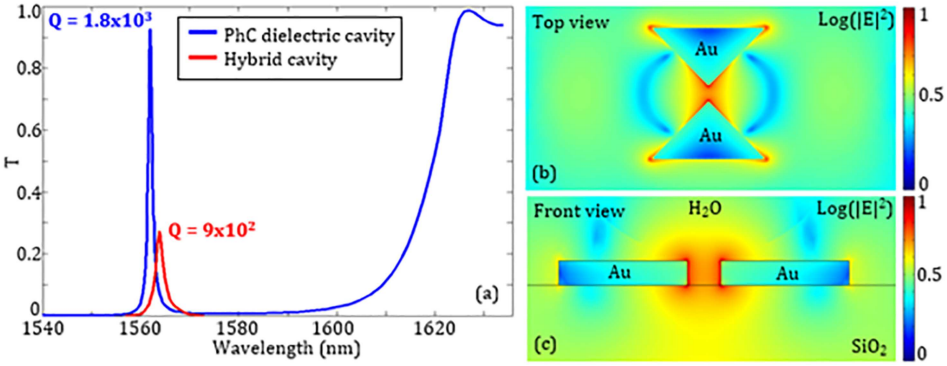

FIG. 2. (a) Transmission spectrum of the 1D PhC dielectric cavity (blue curve) and hybrid cavity (red curve); (b) top view and (c) cross-section of the hybrid cavity at resonance.

their height in order to obtain a resonance peak close to 1550 nm. A gap of s = 40 nm was found to be the best compromise between strong energy confinement and low optical loss in the plasmonic cavity. Losses decrease as the gap becomes larger, at the expense of energy confinement. The total length of the nanoantenna is therefore 480 nm, which almost corresponds to the width of the Si nanowire [Fig. 1(b)]. The Lorentz-Drude model[30] was used to determine the gold permittivity.

We have also simulated the behavior of the single bowtie nanoantenna in water and placed on a silica substrate. A TE-polarized plane wave has been assumed in input at the nanoantenna from the silica substrate, in order to simulate the same coupling condition that is obtained in the hybrid cavity between the PhC cavity and the bowtie.

A Q-factor ≈ 5 and a mode volume $V = 5 \times 10^{-4}$ $(\lambda/n)^3$, which is a typical value for a plasmonic nanoantenna and corresponds to $Q/V \sim 10^4$ $(\lambda/n)^{-3}$. The results get more interesting as we put the two cavities together, as shown in Figs. 1 and 2. For such a hybrid cavity, the Q-factor only drops by a factor 2 compared to the PhC cavity (from Q = 1800 to 900); the transmission drops by a factor 3.6 to T = 26%. The mode volume remains almost unaltered to that of the single nanoantenna and we calculate $V = 6 \times 10^{-4}$ $(\lambda/n)^3$. This results in a remarkably high $Q/V = 1.5 \times 10^6$ $(\lambda/n)^{-3}$ and a strong energy confinement in the bowtie. The steep optical gradient in the bowtie gap [Figs. 2(b) and 2(c)] then makes the hybrid cavity very suitable for optical trapping applications.

We have also simulated the hybrid device performance with a displacement between the bowtie and the PhC, in order to take into account possible issues for the fabrication tolerances. We have obtained a decrease of the values of the optical force of about 10% with a shift of the bowtie up to 50 nm in both in-plane directions, which is a value that can be controlled by the conventional fabrication processes used to realize the hybrid cavity. This also confirms a high value of the optical stability, which still provides a long trapping time as required to the nanotweezer.

DEVICE FABRICATION

For the experimental demonstration, we used an SOI wafer with a 220 nm thick device layer and a 3 μm thick buried oxide layer. Electron-beam lithography with a Raith "Voyager" system was used to define the pattern in AR-P 6200.13 resist according to our standard recipe and then dry etched (see S2 of the supplementary material). The cavity was then attached to a microchannel of Polydimethylsilaxane (PDMS) to control the water flow in the medium surrounding the device. Micrographs of a fabricated device are shown in Fig. 3.

EXPERIMENTAL RESULTS

An end-fire setup was used to characterize the hybrid cavity (see S3 of the supplementary material). The experimental transmission spectrum of the hybrid cavity, shown in Fig. 4(a), has been

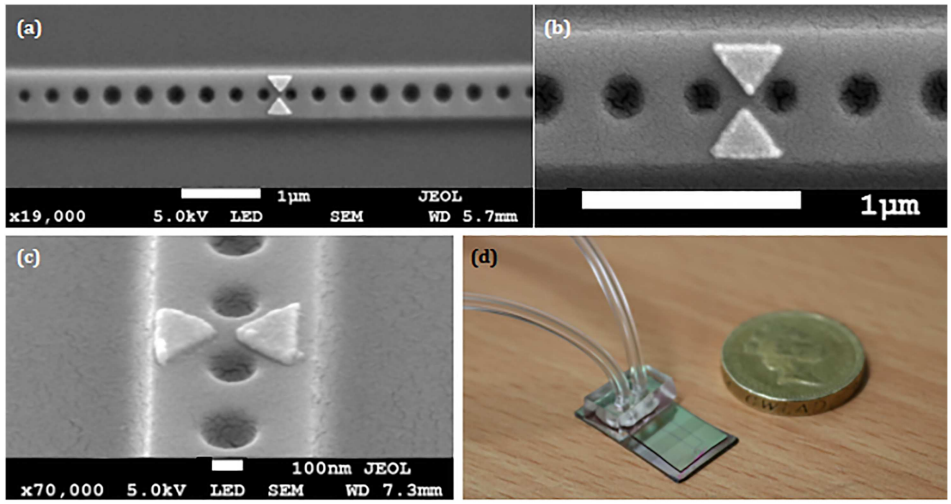

FIG. 3. (a) SEM micrograph of the cavity with [(b) and (c)] a higher magnification view of the bowtie nanoantenna demonstrating good alignment with the PhC cavity; (d) Photograph of the assembled optofluidic chip with the PDMS microchannel bonded to the photonic/plasmonic cavity.

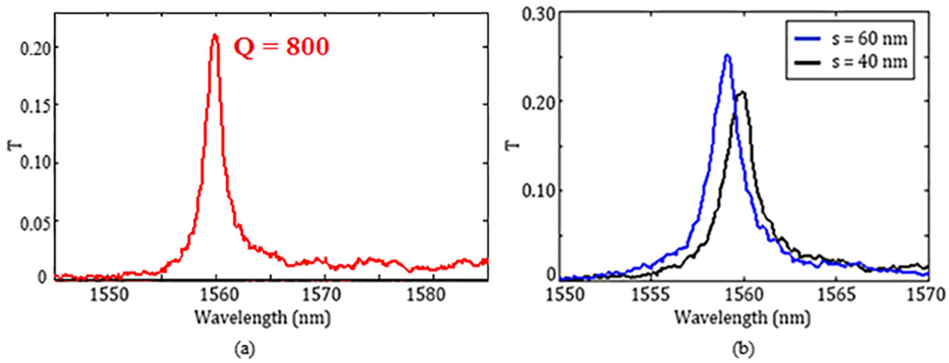

FIG. 4. (a) Transmission of the cavity with a bowtie slot size $s = 40$ nm; (b) experimental spectra of the hybrid cavity with the same PhC structure for two different values of the bowtie slot size s.

normalized to that of a simple nanowire to obtain the on-chip value of transmission. Experiments confirm a value of $Q = 1700$ and $T = 90\%$ for the PhC cavity, while the hybrid cavity exhibits a Q of 800 and a $T = 22\%$. Note the excellent agreement with the simulation curves of Fig. 2(a), which includes the observed 1 nm red-shift of the resonance due to the higher effective index caused by the presence of the bowtie.

The position of the bowtie nanoantenna and its separation from the PhC structure strongly affect the performance of hybrid cavity. The energy in the bowtie at resonance, calculated by 3D FEM simulations, is around 4% of the total amount of energy in the whole device with $G = 130$ nm. A thinner gap between the bowtie and the PhC cavity could be used to improve the vertical coupling efficiency, so obtaining an enhancement of the energy in the bowtie by a factor 2 with $G = 50$ nm (to ~8%). However, this improvement would be traded off against a significant reduction in the resonance transmission to $T \sim 5\%$, which we did not consider acceptable.

The energy confinement in the bowtie also depends on the gap with s. When s decreases from $s = 60$ nm to $s = 40$ nm, the transmission and Q factor slightly decrease, but the energy density in the bowtie goes up, which is reflected by the increase in the Q/V from 1.1×10^6 $(\lambda/n)^{-3}$, with $s = 60$ nm, to 1.3×10^6 $(\lambda/n)^{-3}$, with $s = 40$ nm. This suggests that reducing s is beneficial, but given the added complexity of realizing the bowtie on top of a waveguide and requiring high yield, we found that $s = 40$ nm was a realistic lower bound for the gap width.

HYBRID CAVITY TWEEZER PERFORMANCE

The high Q/V value combined with the strong energy confinement in the bowtie's hotspot and the fact that the hotspot is placed outside the cavity are fundamental features of the hybrid cavity that are very favorable for optical trapping applications. In particular, these features are advantageous for the trapping of nanoscale particles ($a << \lambda$), which are more difficult to trap than microscale ($a \sim \lambda$) particles, because optical forces scale as the third power of the particle radius.[31–34]

In order to assess the tweezing performance of the hybrid cavity, we performed 3D FEM simulations and calculated the optical forces exerted by the hybrid cavity on 100 nm polystyrene and Au beads, using the Maxwell Stress Tensor (MST) method.[35]

Our results confirm the high values of optical force generated by the cavity. The trapping efficiency is typically described by the optical stability S and the optical stiffness k. The stability is defined as $S = U/k_B T_c$, where U $(= \int_{r_0}^{\infty} (F_{tot} dr))$ is the potential energy that corresponds to the work required to bring the nanoparticle from a free position to the trapping site, k_B is the Boltzmann constant, and T_c is the temperature expressed in K.[36] The requirement for a stable trapping condition is $S > 10$, which ensures that the potential energy U is significantly higher than the thermal energy $k_B T_c$, such that the trapping force is strong enough to completely overcome the Brownian motion of the particle.[20,37] This condition also highlights the need for high values of U with low input power, in order to keep the temperature low and not to affect the trapping efficiency by adding Brownian motion. The optical stiffness k ($=F/x$ with F the optical force and x the particle position) is related to the strength of the restoring force towards the equilibrium point in the bowtie gap; high values of k facilitate the attraction of the particle and make it more difficult to push the particle away from the trapping site.[38]

For an input power of 1 mW into the cavity, we calculate an optical force of order pN exerted by the cavity onto the particle. This value corresponds to an optical stability of $S = 12$ for a 100 nm polystyrene bead and $S = 44$ for a 100 nm Au bead, respectively. The trap stiffness is $k = 40$ pN/(nm W) for the dielectric particle and $k = 70$ pN/(nm W) for the metal one. By comparison, we calculate a stability $S << 10$ for the dielectric cavity alone, which highlights the advantage of the hybrid approach and its higher Q/V value.

The proposed configuration has a remarkable advantage if compared to the performance shown by other hybrid nanotweezers in the literature. As an example, Ref. 20 reports on a bowtie nanoantenna vertically coupled to an optical waveguide. The addition of the photonic crystal cavity, as in this work, allows increasing the Q-factor, achieving at the same time a stronger light confinement. Reference 20 reports lower theoretical values of both optical force and trapping stiffness with respect to those obtained by the configuration we propose, which also provides high values of the resonance transmission ($T > 25\%$), corresponding to a good detection resolution for trapping events.

We have also calculated by 3D FEM simulations the hybrid tweezer performance for trapping a 200 nm Au bead, which is the condition considered in the experiments. As expected, a decrease of the resonance transmission up to $T = 2\%$ has been calculated in presence of a trapping event of a single 200 nm Au bead (see Fig. 5).

As confirmed by the Rayleigh approximation, an enlargement of the target object corresponds to higher values of optical forces, with an improvement of the peak values of optical force up to $F \sim 10$ pN, which corresponds to a high value of stability S ($S > 10$) for power values $P_{in} < 200$ μW.

EXPERIMENTAL

We now confirm the trapping efficiency of the hybrid cavity using 200 nm Au beads. The Au nanoparticles were dispersed in an aqueous solution with a concentration of 1.9×10^9 particles/ml. The fluidic flow was controlled by a microfluidic pump to ensure laminar flow. A tunable laser was used as the light source and we pre-compensated for the expected red-shift of the resonance [Fig. 6(b)]. We used a laser power $P_{las} = 8$ mW. The power measured by the output photodetector is $P_{out} = 4.8$ μW and, therefore, due to symmetry, the power in the cavity is estimated to be $P_{cav} = \sqrt{P_{las} \cdot P_{out}}$ = 190 μW.[39] Once a particle flows very close to the bowtie, the gradient force draws the bead towards the cavity, which results in a stable trapping condition (see Fig. 7).

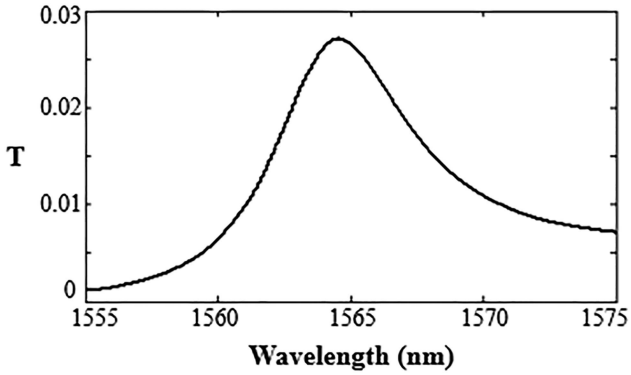

FIG. 5. Transmission spectrum of the hybrid cavity after the trapping of a 200 nm Au bead.

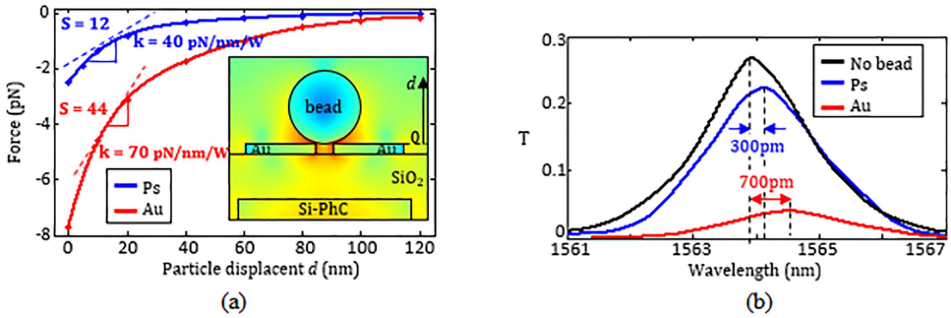

FIG. 6. (a) Optical forces exerted on a 100 nm polystyrene (blue line) and an Au (red line) nanoparticle as a function of the vertical distance from the cavity. (b) Transmission spectra of the hybrid cavity without (black line) and with a 100 nm polystyrene (blue line) and an Au (red line) trapped bead. The resonance condition is red-shifted by a wavelength difference of approximately $\Delta\lambda$ = 300 pm and $\Delta\lambda$ = 700 pm due to the presence of the polystyrene and the Au beads, respectively.

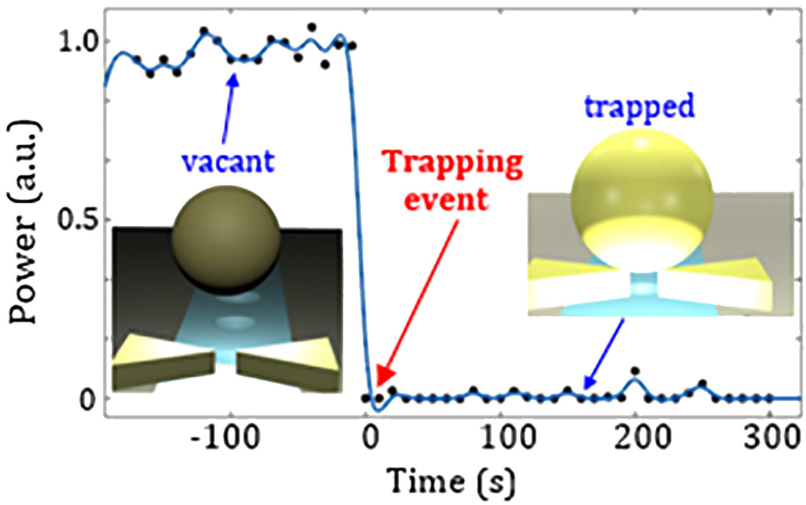

FIG. 7. Power at the output of the hybrid cavity experimentally observed in time. The transmission strongly drops at t = 0 s when a trapping event of a single 200 nm Au bead does occur. The trapping condition maintains stable t > 5 min with P_{cav} = 190 μW. The position of the bead with respect to the bowtie is also sketched.

Even though we had pre-compensated for the expected red-shift of the resonance by setting the tuneable laser accordingly, a strong decrease of the transmission is observed at t = 0 s (see Fig. 5)

when a trapping event occurs, due to the absorption and scattering by the gold nanoparticle, as confirmed by simulations [see Fig. 6(b)].

This behavior confirms the ease of detection of a trapping event by observing the change in transmission. The strength of the optical trap is confirmed by the observation that only very weak oscillations in transmission following the trapping event ($t > 0$ s) are observed, which indicate the high trap stiffness calculated by 3D FEM simulations and correspondingly the reduced Brownian motion. We have also attempted to use the 1D cavity without bowtie for the same input optical power but did not observe any particle deflection or trapping, again highlighting the benefit of the hybrid geometry.

The minimum size of the beads used to verify the trapping efficiency of the photonic/plasmonic cavity is 200 nm. An optical setup different from that used for those experiments (see S3 of the supplementary material) is required to observe a trapping event of a smaller dielectric bead (i.e., a bead's size $\leq$ 100 nm), due to less evident changes in resonance wavelength and resonance transmission.

In the literature, high trapping efficiency has been verified with plasmonic tweezers, providing trapping also at nanoscale. For instance, trapping of 50 nm dielectric beads with a near-field nanotweezer realized by mounting a plasmonic bowtie onto the tip of a fiber has been demonstrated in Ref. 40. The hybrid structure proposed in this work is clearly different: as already discussed before, its key characteristic is that the combined photonic/plasmonic cavity provides a trapping stiffness that is higher than in a simple plasmonic configuration with a stronger restoring force on the bead in the trapping site. This behaviour is confirmed by the weak oscillations after having trapped the bead in the equilibrium point, compared to the behaviour described in Ref. 40. Furthermore, a lower power is required which is important to minimise heating effects.

In conclusion, our results represent the first demonstration of a hybrid photonic crystal/bowtie plasmonic resonator cavity with in-plane light propagation, a geometry that enables the integration of nanotweezers into an on-chip system. We demonstrate high transmission and high efficiency optical trapping, based on the observed ultra-high Q/V ($>10^6$ $(\lambda/n)^{-3}$) ratio of the device, the highest value reported for a hybrid cavity reported to date. The ability to confine a high fraction of the optical energy in the hotspot outside the cavity affords direct interaction with an analyte and increases the sensitivity for sensing applications. Moreover, the high transmission ($T > 20\%$) makes possible to detect any changes in the resonance condition simply and easily.

SUPPLEMENTARY MATERIAL

See S1 of the supplementary material for the configuration of the photonic/plasmonic cavity with the description of the whole geometrical parameters to realize the PhC cavity and the bowtie nanoantenna. In S2, all fabrication steps to realize the optofluidic chip with the hybrid cavity integrated in a microfluidic channel have been described. In S3, we show the optical setup used for the optical characterization of the photonic/plasmonic cavity based on an end-fire technique.

[1] Y. Akahane, T. Asano, B.-S. Song, and S. Noda, Nature **425**, 944 (2003).
[2] P. B. Deotare, M. W. McCutcheon, I. W. Frank, M. Khan, and M. Loncar, Appl. Phys. Lett. **94**, 121106 (2009).
[3] R. De La Rue, H. Chong, M. Gnan, N. Johnson, I. Ntakis, P. Pottier, M. Sorel, A. Md Zain, H. Zhang, E. Camargo, C. Jin, M. Armenise, and C. Ciminelli, New J. Phys. **8**, 256 (2006).
[4] B. J. M. Hausmann, B. J. Shields, Q. Quan, Y. Chu, N. P. de Leon, R. Evans, M. J. Burek, A. S. Zibrov, M. Markham, D. J. Twitchen, H. Park, M. D. Lukin, and M. Loncar, Nano Lett. **13**, 5791 (2013).
[5] C. Monat, C. Grillet, M. Collins, A. Clark, J. Schroeder, C. Xiong, J. Li, L. O'Faolain, T. F. Krauss, B. J. Eggleton, and D. J. Moss, Nat. Commun. **5**, 3246 (2014).
[6] M. J. Burek, Y. Chu, M. S. Z. Liddy, P. Patel, J. Rochman, S. Meesala, W. Hong, Q. Quan, M. D. Lukin, and M. Loncar, Nat. Commun. **5**, 5718 (2014).
[7] M. G. Scullion, A. Di Falco, and T. F. Krauss, Biosens. Bioelectron. **27**, 101 (2011).
[8] S. Mandal, X. Serey, and D. Erickson, Nano Lett. **10**, 99 (2010).
[9] K. J. Vahala, Nature **424**, 839 (2003).
[10] Q. Quan and M. Loncar, Opt. Express **19**, 18529 (2011).
[11] H. Sekoguchi, Y. Takahashi, T. Asano, and S. Noda, Opt. Express **22**, 916 (2014).
[12] D. K. Gramotnev and S. I. Bozhvolnyi, Nat. Photonics **4**, 83 (2010).
[13] M. Kuttge, F. J. G. de Abajo, and A. Polman, Nano Lett. **10**, 1537 (2010).

[14] K. J. Russel and E. L. Hu, Appl. Phys. Lett. **97**, 163115 (2010).
[15] F. De Angelis, M. Patrini, G. Das, I. Maksymov, M. Galli, L. Businaro, L. C. Andreani, and E. Di Fabrizio, Nano Lett. **8**, 2321 (2008).
[16] M. Barth, S. Schietinger, S. Fischer, J. Becker, N. Nüsse, T. Aichele, B. Löchel, C. Sönnichsen, and O. Benson, Nano Lett. **10**, 891 (2010).
[17] D. Conteduca, F. Dell'Olio, F. Innone, C. Ciminelli, and M. N. Armenise, Opt. Laser Technol. **77**, 151, (2016).
[18] N. P. de Leon, B. J. Shields, C. L. Yu, D. E. Englund, A. V. Akimov, M. D. Lukin, and H. Park, Phys. Rev. Lett. **108**, 226803 (2012).
[19] M. Mossayebi, A. J. Wright, A. Parini, M. G. Somekh, G. Bellanca, and E. C. Larkins, Opt. Quant. Electron. **48**, 275 (2016).
[20] P.-T. Lin, H.-Y. Cinput Hu, T.-W. Lua, and P.-T. Lee, Lab Chip **14**, 4647 (2014).
[21] C. Ciminelli, D. Conteduca, F. Dell'Olio, and M. N. Armenise, IEEE Photonics J. **6**, 0600916 (2014).
[22] D. Conteduca, F. Dell'Olio, C. Ciminelli, T. F. Krauss, and M. N. Armenise, in 3rd Mediterranean Photonics Conference, MePhoCo, Trani (Italy), 7–9 May 2014.
[23] C.-H. Cho, C. O. Aspetti, J. Park, and R. Agarwal, Nat. Photonics **7**, 285 (2013).
[24] A. El Eter, T. Grosjean, P. Viktorovitch, X. Letartre, T. Benyattou, and F. I. Baida, Opt. Express **22**, 14464 (2014).
[25] M. A. Santiago-Cordoba, M. Cetinkaya, S. V. Boriskina, F. Vollmer, and M. C. Demirel, J. Biophotonics **5**, 629 (2012).
[26] B. J. Roxworthy, K. D. Ko, A. Kumar, K. H. Fung, E. K. C. Chow, G. L. Liu, N. X. Fang, K. C. Toussaint, Jr., Nano Lett. **12**, 796 (2012).
[27] D. Conteduca, F. Dell'Olio, C. Ciminelli, T. F. Krauss, and M. N. Armenise, Appl. Phys. A **122**, 295 (2016).
[28] C. Ciminelli, F. Dell'Olio, D. Conteduca, T. F. Krauss, and M. N. Armenise, in 16th ICTON, Graz, Austria, 6–10 July 2014.
[29] H. Fischer and O. J. F. Martin, Opt. Express **16**, 9144 (2008).
[30] A. D. Rakic, A. B. Djurisic, J. M. Elazar, and M. L. Majewski, Appl. Opt. **37**, 5271 (1998).
[31] K. Svoboda and S. M. Block, Opt. Lett. **19**, 930 (1994).
[32] D. Erickson, X. Serey, Y. F. Chen, and S. Mandal, Lab Chip **11**, 995 (2011).
[33] Y. Pang and R. Gordon, Nano Lett. **12**, 402 (2012).
[34] L. Novotny and B. Hecht, *Principles of Nano-Optics* (Cambridge University Press, New York, 2012).
[35] X. Serey, S. Mandal, and D. Erickson, Nanotechnology **21**, 305202 (2010).
[36] M. Soltani, J. Lin, R. A. Forties, J. T. Inman, S. N. Saraf, R. M. Fulbright, M. Lipson, and M. D. Wang, Nat. Nanotech. **9**, 448 (2014).
[37] C. M. Galloway, M. P. Kreuzer, S. S. Acimovic, G. Volpe, M. Correia, S. Petersen, M. T. Neves-Petersen, and R. Quidant, Nano Lett. **13**, 4299 (2013).
[38] K. C. Neuman and S. M. Block, Rev. Sci. Instrum. **75**, 2787 (2004).
[39] N. Descharmes, U. P. Dharanipathy, Z. Diao, M. Tonin, and R. Houdré, Phys. Rev. Lett. **110**, 123601 (2013).
[40] J. Berthelot, S. S. Aćimović, M. L. Juan, M. P. Kreuzer, J. Renger, and R. Quidant, Nat. Nanotechnol. **9**, 295 (2014).